

# Investigation of the influence of air gap thickness and eccentricity on the noise of the rotating electrical machine

M. Donát<sup>a,\*</sup>

<sup>a</sup>*Institute of Solid Mechanics, Mechatronics and Biomechanics, Faculty of Mechanical Engineering, Brno UT, Technická 2896/2, 616 69 Brno, Czech Republic*

Received 18 September 2013; received in revised form 16 December 2013

---

## Abstract

This article deals with the numerical modelling of the dynamic response of the rotating electrical machine on the application of the magnetic forces. The special attention is paid to the modelling of the magnetic forces that act on the stator winding of the machine and the computational model of the modal properties of the stator winding. The created computational model was used to investigation of the influence of the nominal air gap thickness and the air gap eccentricity on the sound power radiated by outer surface of the stator of the machine. The obtained results show that the nominal air gap thickness has slightly greater influence on the sound power of the machine than eccentricity of the air gap.

© 2013 University of West Bohemia. All rights reserved.

*Keywords:* rotating electrical machine, stator, rotor, magnetic forces, sound power level

---

## 1. Introduction

Magnetic fields in the air gap between the rotor and the stator of the rotating electrical machines induce magnetic forces that act on the machine structure. These forces have character of the time-varying load, which consists of a number of harmonic components different amplitudes and frequencies. The amplitudes and the frequencies of the harmonic components affect among other: a number of pole pairs of the stator winding of the machine, a number of the stator winding slots per pole and phase, a number of the rotor winding slots, saturation effect and last but not least the air gap thickness and the air gap eccentricity.

A computational modelling of the dynamic response of the rotating electrical machine on the magnetic forces is two-stage process. First, the time dependence of the magnetic forces, which act on the stator and the rotor winding, must be obtained. The dynamic response of the machine excited by magnetic forces is calculated in the second step.

Computational models of the magnetic forces can be divided into analytical and numerical. The analytical computational models usually determine the size of magnetic forces based on the geometrical dimensions of the windings of the machine and the amplitude of the first or of the first few harmonics of magnetic flux density. The great advantage of these computational models is their simplicity and a direct physical interpretation. The analytical computational models fail to take into account of some effects which may have, under certain circumstances, a significant influence on the size of the magnetic forces, for example saturation effect of the stator and the rotor winding core, slotting effect, effect of the equalizing currents, which are inducing in the winding in the case of the parallel paths. The analytical computational models are used

---

\*Corresponding author. Tel.: +420 721 511 230, e-mail: Donat.Martin@email.cz.

for example in [10–12, 14]. The numerical computational models determine the size of the magnetic forces from actual distribution of the magnetic field of the machine in each load step; therefore, these computational models are much more complex than analytical computational models and besides saturation effect, slotting effect and effects of the equalizing currents can take into account also losses due to leakage reactance etc. The numerical computational models are consuming computational time; therefore they started to be used more widely in the last decade. The numerical computational models are used for example in [2, 8, 17].

Most of the published studies on the computational modelling of the dynamic behaviour of the rotating electric machines are focused on the examining of the influence of the magnetic forces on the dynamic behaviour of the rotor. The magnetic forces act also on the stator winding. Vibrations of the stator excited by magnetic forces may not have significant effect on the durability of the machine, but may cause excessive noise of the machine; therefore the numerical computational model of the dynamic response of the stator of the rotating electrical machine excited by the magnetic forces is proposed in this paper. This computational model is used to investigation of the influence of the nominal air gap thickness and the air gap eccentricity on the sound power level of the machine.

## 2. Magnetic forces

The computational model of the magnetic forces based on the solution of the coupled electromagnetic problem by finite element method was chosen as the most suitable. This computational model consists of two sub computational models: computational model of the magnetic circuit of the machine and computational model of the electric circuit of the machine. The computational model of the magnetic forces was created in the commercial finite element software ANSYS. In this case ANSYS 14.0 was used. Calculations have been performed for three-phase vertical induction generator; its basic parameters are listed in Table 1.

Table 1. Basic parameters of the machine

Items	Values	Unit
Rated power	380	kW
Rated voltage	6 300	V
Rated current	55	A
Frequency	50	Hz
Number of pole pairs	12	–
Revolutions of the rotor	253	1/min
Outer diameter of the stator winding	1 250	mm
Inner diameter of the stator winding	1 040	mm
Inner diameter of the rotor winding	850	mm
Stator core length	790	mm
Stator slot number	144	–
Rotor slot number	176	–
Connection of the stator windings coils	Y	–

### 2.1. Fundamental equations

The computational model of the magnetic circuit of the machine assumes that the magnetic field is constant along the centreline of the stator. This assumption reduces number of degrees

of freedom of this computational model significantly, because it is not necessary to create three-dimensional model of the magnetic circuit of the machine but merely two-dimensional. Eq. (1) describes the distribution of the magnetic field in the two-dimensional region

$$\nabla \times (\nu \nabla \times \mathbf{A}) - \gamma \frac{\partial \mathbf{A}}{\partial t} + \frac{N_S}{S_S} \mathbf{I}_S + \frac{\sigma}{l_R} \mathbf{U}_R = \mathbf{0}. \quad (1)$$

This equation can be derived from Maxwell equations and constitutive relations describing material properties, as [5] shows. Here  $\mathbf{A}$  is the magnetic vector potential,  $\mathbf{I}_S$ ,  $\mathbf{U}_R$  are column vectors of the currents of the stator winding and electric potential differences of the rotor bars,  $N_S$  is the number of turns in series in each coil of the stator winding  $S_S$  is the cross section of the stator coil,  $l_R$  is the length of the rotor bar. Time is denoted as  $t$ ,  $\nu$  and  $\gamma$  are magnetic reluctivity and electric conductivity. The stator winding of the machine is connected to the line voltage that is source of the magnetic field and magnetic field of the stator causes the rotor currents; therefore the stator voltage equation

$$\mathbf{R}_S \mathbf{I}_S + \frac{l_S N_S}{S_S} \iint_{S_S} \frac{\partial \mathbf{A}}{\partial t} dS - \mathbf{U}_S = \mathbf{0} \quad (2)$$

and rotor voltage equation

$$\mathbf{R}_R \mathbf{I}_R + \mathbf{R}_R \sigma \iint_{S_R} \frac{\partial \mathbf{A}}{\partial t} dS - \mathbf{U}_R = \mathbf{0} \quad (3)$$

must be coupled with the magnetic field equation (1). In these equations  $\mathbf{U}_S$ ,  $\mathbf{I}_R$  are column vectors of the electric potential differences of the stator coils and currents of the rotor bars,  $\mathbf{R}_S$ ,  $\mathbf{R}_R$  are the matrices of DC resistances of the stator coils and the rotor bars.

The electrical circuit of the rotor cage consists of the rotor bars ( $L_R$ ) and shorting rings. The shorting rings are divided into segments; each segment connects the ends of two adjacent bars and is modelled by a ring segment resistance ( $R_i$ ) and a ring segment inductance ( $L_i$ ), as Fig. 1 shows. Two equations are obtained by application of Kirchhoff's Laws for electrical circuit of the rotor cage

$$\mathbf{I}_{\text{ring}} - \mathbf{M} \mathbf{I}_R = \mathbf{0}, \quad (4)$$

$$\mathbf{M} \mathbf{U}_R + \mathbf{R}_{\text{ring}} \mathbf{I}_{\text{ring}} + \mathbf{L}_{\text{ring}} \frac{d}{dt} \mathbf{I}_{\text{ring}} = \mathbf{0}, \quad (5)$$

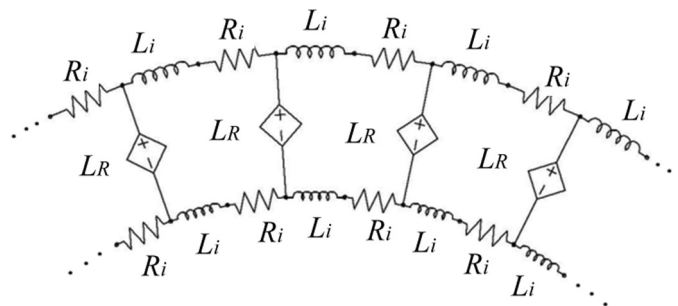


Fig. 1. Electrical circuit of the rotor

where  $\mathbf{M}$  is the connection matrix associated with the rotor cage,  $\mathbf{I}_{\text{ring}}$  is the column vectors of the ring segments currents,  $\mathbf{R}_{\text{ring}}$  and  $\mathbf{L}_{\text{ring}}$  are the matrices of the ring segments resistances and the ring segments inductances.

According to [3], the ring segment resistance and the ring segment inductance can be calculated from Eqs. (6) and (7)

$$R_i = \rho_c \frac{l_i}{A_i}, \tag{6}$$

$$L_i = \mu_0 l_i \lambda_i, \tag{7}$$

where  $\rho_c$  is the electrical resistivity of the ring segment,  $l_i$  is the median length of the ring segment,  $A_i$  is the area of the ring segment cross section,  $\mu_0$  is the permeability of air and  $\lambda_i$  is the geometrical permeance of the ring segment, which can be calculated from Eq. (8)

$$\lambda_i \approx \frac{6D_r}{4N_r L_r \sin^2\left(\frac{\pi p}{N_r}\right)} \log\left(\frac{D_r}{2(a+b)}\right). \tag{8}$$

Here  $D_r$  is the median diameter of the shorting ring,  $N_r$  is the number of rotor bars,  $L_r$  is the length of the rotor winding core,  $p$  is the number of the pole pairs,  $a$  is the cross section height of the shorting ring and  $b$  is the cross section width of the shorting ring.

Eqs. (1)–(5) create computational model

$$\begin{bmatrix} \mathbf{K}_{11}(\mathbf{A}) & \mathbf{K}_{12} & \mathbf{K}_{13} & 0 & 0 \\ \mathbf{K}_{21}(\mathbf{A}) & \mathbf{K}_{22} & 0 & 0 & 0 \\ \mathbf{K}_{31}(\mathbf{A}) & 0 & \mathbf{K}_{33} & \mathbf{K}_{34} & 0 \\ 0 & 0 & 0 & \mathbf{K}_{44} & \mathbf{K}_{45} \\ 0 & 0 & \mathbf{K}_{53} & 0 & \mathbf{K}_{55} \end{bmatrix} \cdot \begin{bmatrix} \mathbf{A} \\ \mathbf{I}_S \\ \mathbf{U}_R \\ \mathbf{I}_R \\ \mathbf{I}_{\text{ring}} \end{bmatrix} = \begin{bmatrix} \mathbf{0} \\ \mathbf{U}_S \\ \mathbf{0} \\ \mathbf{0} \\ \mathbf{0} \end{bmatrix} \tag{9}$$

with the unknowns  $\mathbf{A}$ ,  $\mathbf{I}_S$ ,  $\mathbf{U}_R$ ,  $\mathbf{I}_R$ ,  $\mathbf{I}_{\text{ring}}$  and the source vector  $\mathbf{U}_S$ . This computational model is solved by time-stepping finite element method. More information about this computational model can be found for example in [1, 2, 4, 5]. The electromagnetic forces acting on the winding of the machine can be calculated from distribution of the magnetic field in the air gap for example by Maxwell stress tensor method [4]

$$\mathbf{F}_{el-mag} = \frac{1}{\mu_0} \int_s \begin{bmatrix} B_x^2 - \frac{1}{2}B^2 & B_x B_y \\ B_x B_y & B_y^2 - \frac{1}{2}B^2 \end{bmatrix} \mathbf{n} ds, \tag{10}$$

where  $B_x$  and  $B_y$  are the components of magnetic flux density in Cartesian coordinate system,  $B = \sqrt{B_x^2 + B_y^2}$  and  $\mathbf{n}$  is unit-vector normal to the boundary  $s$ .

## 2.2. Finite element model of the magnetic circuit of the machine

Fig. 2 shows the model of the geometry of the magnetic circuit of the machine. The frame of the stator does not have a significant effect on the distribution of the magnetic field inside the machine; hence the stator is represented by the stator pack in this computational model only.

The stator winding core and the rotor winding core are made of electrical steel M400-50A. This material is characterized by nonlinear dependence of the magnetic flux density on the magnetic field intensity, which is described by B-H curve in Fig. 3. The magnetic behaviour of the other materials has been described by relative permeability. The material characteristics of

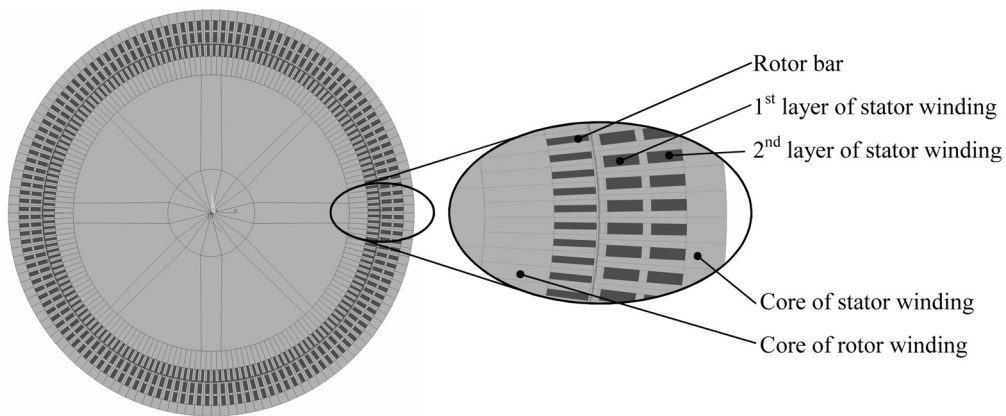


Fig. 2. Model of the geometry of the magnetic circuit of the machine

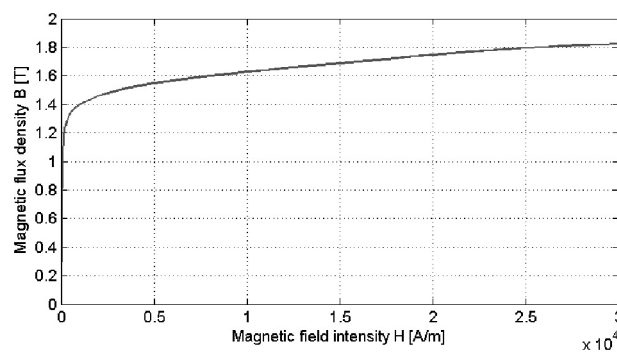


Fig. 3. B-H curve of electrical steel M400-50A

Table 2. Material characteristics: Relative permeability, Electrical resistivity

Item	Material	$\mu_r$ [-]	$\zeta$ [ $\Omega\text{m}$ ]
Stator winding	Cooper	0.999 99	$1.72 \cdot 10^{-8}$
Rotor bars	Cooper	0.999 99	$1.72 \cdot 10^{-8}$
Wedges	Sklotextit g10	1.0	–
Rotor shaft	Steel	8 000	–
Others	Air	1	–

the rotor bars and the stator windings are supplemented by the electrical resistivity. The material characteristics are presented in Table 2.

The model of the geometry was discretized by PLANE53 elements, which are intended for low-frequency electromagnetic analysis. The air gap between the stator and the rotor of the machine was divided into two parts. The part of the air gap adjacent to the rotor was discretized with the rotor. The part of the air gap adjacent to the stator was discretized with the stator. The finite element mesh of the rotor and the stator was generated separately in order to ensure a relative motion of the rotor due to the stator. Both meshes were coupled by constraint equations. The largest gradient of the magnetic potential is expected in the air gap; therefore the finite element mesh is here the densest.

The rotor bars were discretized by kind of the PLANE53 element that is intended for massive conductors. The coils of the stator winding were discretized by kind of the PLANE53 element that is intended for stranded coils. Other parts of the magnetic circuit of the machine were discretized by basic version of the PLANE53 element.

### 2.3. Finite element model of the electrical circuit of the machine

Elements CIRCUI24 are used for modelling the electrical circuits in ANSYS. Fig. 4 shows the electrical circuit of the stator winding of the machine. This circuit consists of the three-phase voltage source ( $U, V, W$ ) and the stator coils ( $L_S$ ). The electrical circuit of the rotor has been described in the paragraph 2.1. The part of the electrical circuit of the rotor Fig. 1 shows.

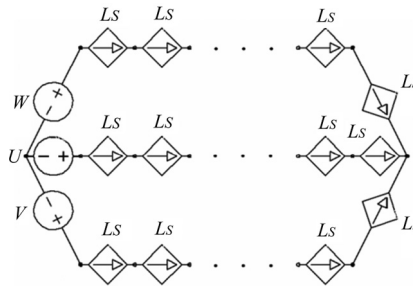


Fig. 4. Electrical circuit of the stator

### 3. Coupling of the magnetic circuit with the electrical circuit

According to [1] the ANSYS software allows a direct coupling between the magnetic circuit model and the electrical circuit model of the machine. The element PLANE53, which was used for discretization of the rotor bars, has three degrees of freedom per node: a magnetic potential, an electric current passing through the rotor bar (CURR) and an electrical potential drop between the ends of the rotor bar (EMF). The elements CIRCUI24, which represent the rotor bars in the electrical circuit of the rotor, are determined by three nodes, as Fig. 5 shows. The nodes I and J are the nodes of electrical circuit and have one degree of freedom a voltage. The node K has two degrees of freedom: CURR and EMF. This node is identical with the arbitrarily chosen node of the area, which represents the appropriate rotor bar in the magnetic circuit of the machine. The CIRCUI24 element represents the rotor bar as a whole. Thus, all nodes of the rotor bar region must be coupled in the magnetic circuit of the machine in CURR degree of freedom and EMF degree of freedom. The same procedure must be used for coupling the stator windings coils in the electrical circuit model with the magnetic circuit model.

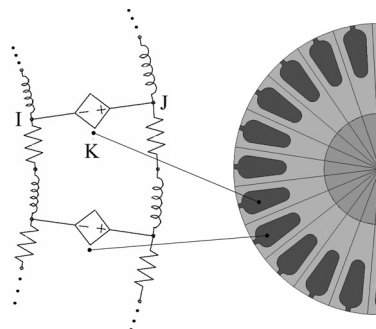


Fig. 5. Coupling of the magnetic circuit with the electrical circuit

### 3.1. Solution of the electromagnetic problem and calculation of the magnetic forces

ANSYS software allows solving electromagnetic problems by nonlinear time-harmonic analysis or by time-stepping method. According to [1], the nonlinear time-harmonic analysis is less time-consuming than time-stepping analysis. In case of the nonlinear time-harmonic analysis, the rotor of the machine is treated as a stationary and the relative motion of the rotor with respect to the stator is taken into account by slip transformation. The essence of the slip transformation is explained in [2, 18] and is based on the change of the rotor cage resistance depending on the slip. This approach takes into account harmonics related with the supply voltage and winding construction only, but harmonics related with the rotor motion are ignored; hence the solution of the created task was performed time-stepping method. A length of the time step was used  $4 \cdot 10^{-5}$  s and the constraint equations, which coupled the finite element mesh of the rotor and the stator, were modified at the end of each time step to match the rotation of the rotor during the time step.

The magnetic forces acting on the winding were calculated from distribution of the magnetic field in the air gap of the machine by Maxwell stress tensor method that is directly implemented in ANSYS.

### 3.2. Results

The type of the air gap eccentricity considered in this article is in Fig. 6. Proposed computational model was programmed parametrically by ADPL language commands. This approach enabled easy modification of the nominal air gap thickness  $g_0$  and the parameter of the air gap eccentricity  $\delta$ , which is defined as  $\delta = x_{ex}/g_0$ . The time dependence of the magnetic forces, which act on the stator winding of the machine, was calculated for nominal air gap thickness  $g_0 = 1.2, 1.0$  and  $0.8$  mm and values of parameter  $\delta = 0, 0.2$  and  $0.4$ . Figs. 7 and 8 show the part of this dependence for values of parameters  $g_0 = 1.2$  mm,  $\delta = 0$  and  $g_0 = 1.2$  mm,  $\delta = 0.4$ . The influence of the air gap eccentricity on the distribution of the electromagnetic forces along the stator winding can be seen from these figures. The magnetic forces are periodically distributed along the stator winding in the case of the machine with the symmetric air gap. In the case of the air gap eccentricity, the magnetic forces increase in the vicinity of the minimal air gap thickness and decrease in the vicinity of the maximal air gap thickness, as Fig. 8 shows.

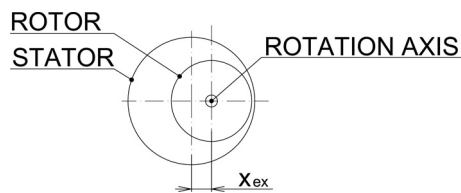


Fig. 6. Type of the air gap eccentricity

## 4. Dynamic response of the stator on the electromagnetic forces

The time dependences of the magnetic forces, which were obtained in the previous step, were used to investigation of the influence of the air gap thickness and the air gap eccentricity on the sound power level radiated by the outer surface of the stator of the machine. The dynamic response of the stator of the machine on the electromagnetic forces was calculated as first. The sound power level radiated by outer surface of the stator was calculated from this response. The calculations were carried out in ANSYS again.

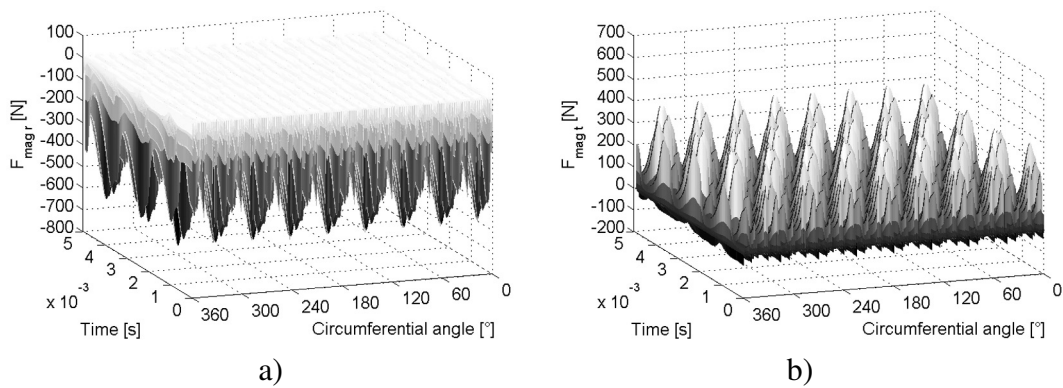


Fig. 7. Part of the time dependence of the magnetic forces:  $g_0 = 1.2 \text{ mm}$ ,  $\delta = 0$ , a) radial component of the magnetic forces, b) tangential component of the magnetic forces

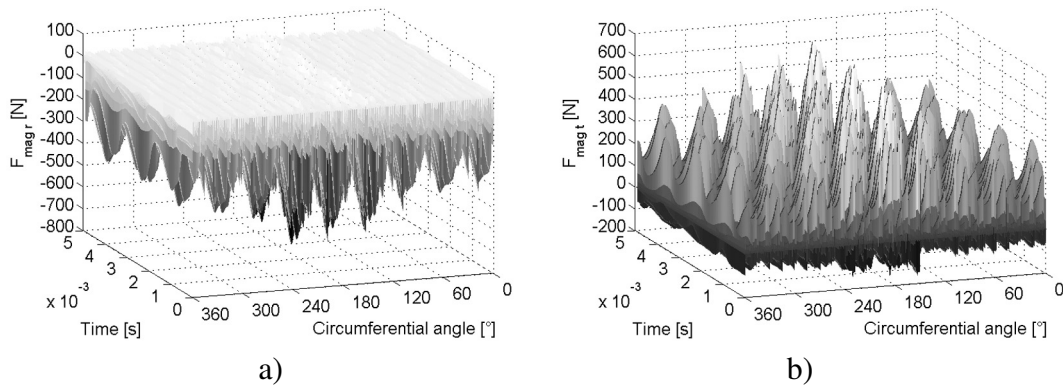


Fig. 8. Part of the time dependence of the magnetic forces:  $g_0 = 1.2 \text{ mm}$ ,  $\delta = 0.4$ , a) radial component of the magnetic forces, b) tangential component of the magnetic forces

#### 4.1. Dynamic response of the stator excited by electromagnetic forces

Fig. 9 shows the model of the geometry of the stator of the machine. This model was created with regard to the modal properties of the stator of the real machine; therefore covers of the ventilation holes, holes for mounting of the generator in the machine room and other parts that do not have significant influence on the total stiffness of the stator were not modelled.

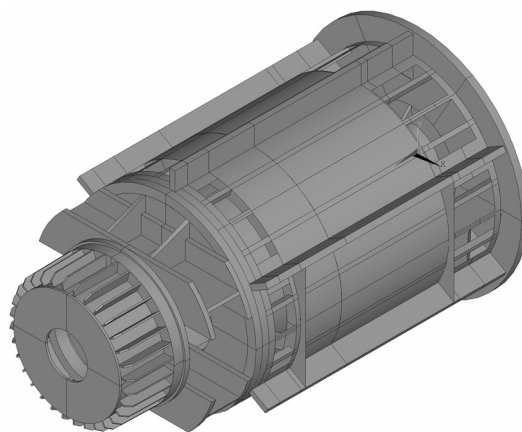


Fig. 9. Model of the geometry of the stator

A frame and shields of the stator are weldments made of a structural steel. A mechanical behaviour of this material was described by constitutive relations that assume a homogeneous isotropic linear elastic behaviour of this material. A stator pack consists of stator sheets with slots for a stator winding. Stator winding is placed in two layers in the slots. Each layer is formed by eight rectangular copper rods. These rods are separated by a layer of insulating varnish Utimeg 2000. The stator winding is covered by a resin Nomex E56 and ensured by the wedges in the stator winding slots. Detailed treatment of the stator pack would result in a very long computational time of the dynamic response of the stator; therefore the stator winding is modelled as the hollow cylinder made of the homogenous isotropic linear elastic material in practise [9, 13, 16]. The main idea of this approach is to replace the stator pack by the simple body with similar modal properties in the radial direction. The modal properties in the axial direction are not important, because magnetic force component in this direction is not significant. The publications [9, 13, 16] do not describe a process for determining the material characteristic of the stator pack replacement. Experimental modal analysis of the stator pack is not available too. Hence the procedure proposed in [7] was used. The natural frequencies of the stator pack in radial direction can be calculated approximately by the computational modal analysis of the two dimensional model of the stator pack cross section with detailed treatment of the stator winding. Procedure for calculating of the material characteristics of the stator pack replacement is as follows. The Poisson ratio does not have a significant influence on the modal properties of the stator pack replacement; hence it was set to typical value 0.3. The density of material of the stator pack replacement was calculated from the ratio of the weight of the real stator pack and the volume of the stator pack replacement. The computational modal analysis of the cross section of the stator pack replacement was performed in the next. The tensile modulus of the stator pack replacement was searched so that the first two natural frequencies of the stator pack replacement were as closed as possible to the first two natural frequencies of the real stator pack. Naturally, calculation accuracy is affected by several uncertainties. The most significant uncertainty is probably assumption of the homogenous isotropic material behaviour. However this approach is the simplest way to determine tensile modulus of the stator pack replacement. Material characteristics used in calculation of the stator pack replacement are presented in Table 3.

Table 3. Material characteristics: Density, Tensile modulus, Poisson ratio

Item	Material	$\rho$ [kg · m <sup>-3</sup> ]	E [Pa]	$\mu$ [-]	Reference
Frame, shields	Structural steel	7 850	$2.1 \cdot 10^{11}$	0.30	
Stator sheets	M400-50A	7 700	$2.1 \cdot 10^{11}$	0.30	[15, 19]
Stator winding	Cooper	8 960	$1.2 \cdot 10^{11}$	0.35	
Insulation varnish	Utimeg 2000	1 090	$3.45 \cdot 10^9$	0.40	[15]
Resin	Nomex E56	670	$2.46 \cdot 10^9$	0.40	[15]
Wedges	Sklotextit G11	1 900	$1.05 \cdot 10^{10}$	0.41	[15]
Replacement of stator pack		6 227	$2.84 \cdot 10^{10}$	0.30	

A casing of the generator was discretized by SHELL181 elements, other parts of the stator were discretized by SOLID185 elements. The finite element mesh was created with respect to the evenness of the mesh.

Loading of the stator winding by the magnetic forces was modelled prescribing the time-varying forces to the nodes on the inner surface of the replacement of stator pack. These time-

varying forces were determined on the basis of the time dependences of the magnetic forces, which were obtained in the previous chapter. It must be remembered that the time dependences of the magnetic forces are related to the unit length of the stator pack in this chapter.

The connection of the generator with the base plate in the machine room was modelled by prescribing zero displacements and rotations to the nodes on the contact area of the flange of the generator.

The solution of the dynamic response of the stator excited by magnetic forces was performed in the time domain by Newmark method. A length of the time step was used  $1.6 \cdot 10^{-4}$  s. The initial displacements and velocities of the nodes of the stator are not known; hence were set to zero at the beginning of the calculation. The calculation of the dynamic response had two phases in order suppress of the transients. The gradual loading from zero to full load during first five revolutions of the rotor was used in the first phase. A stabilization of the dynamic response occurred in the second phase of the calculation. This phase lasted for ten revolutions of the rotor.

#### 4.2. Sound power level

The sound power level radiated by outer surface of the stator of the machine was evaluated from the dynamic response of the stator excited by magnetic force. The sound power level was calculated by the basic method that is described in [16]. The sound power radiated by the surface, which is discretized by the finite element mesh, can be calculated from Eq. (11)

$$W_a = \frac{1}{2} \rho_0 c_0 \sigma \sum_{i=1}^N \frac{A_i \bar{v}_{\text{nor } i}^2}{\Pi}, \quad (11)$$

$$\Pi = \sum_{i=1}^N A_i^2, \quad (12)$$

where  $\rho_0$  is the density of the air,  $c_0$  is the speed of the sound in the air,  $\sigma$  is radiation efficiency,  $A_i$  is the surface of the face of the element  $i$  that create outer surface of the stator,  $\bar{v}_{\text{nor } i}$  is the volume velocity of the  $i$ -th face,  $N$  is the number of faces of the element which create outer surface of the stator. The radiation efficiency of the examined machine is not known. According to [6] and [16]  $\sigma = 1$  was used. Naturally, this approach maximizes the estimation of radiated sound power. The volume velocity

$$\bar{v}_{\text{nor } i} = \frac{1}{M} A_i \sum_{j=1}^M v_{\text{nor } ij}, \quad (13)$$

where  $v_{\text{nor } ij}$  is the normal velocity of the  $j$ -th node  $i$ -th face and  $M$  is the number of the nodes that belong the  $i$ -th face of the element. The sound power level is then calculated from Eq. (14)

$$L_{W_a} = 10 \log \frac{W_a}{W_{\text{ref}}}, \quad (14)$$

where  $W_{\text{ref}}$  is the reference value of the sound power. The reference value of the sound power is typically  $1 \cdot 10^{-12} W$ .

### 4.3. Results

The influence of the nominal air gap thickness on the sound power radiated by outer surface of the stator was investigated as first. The machine with the symmetric air gap was considered in these calculations. Fig. 10 shows the time dependence of the sound power level generated by the magnetic forces for the nominal air gap thickness  $g_0 = 1.2, 1.0$  and  $0.8$  mm. It can be said that the decrease of the nominal air gap thickness from 1.2 mm to 1.0 mm leads to increase the sound power level approximately by one to two decibels, which corresponds the increase of the sound power by 25 %, around local minimums even by 75 % as Fig. 11 shows. In the case of the decrease of the nominal air gap thickness from 1.2 mm to 0.8 mm, the sound power increase about 60 %, around local minimums even by 180 %. The increase of the sound power is not too great around the local maximums of the sound power due to saturation effect of the stator core, which reduces the amplitude of the electromagnetic forces.

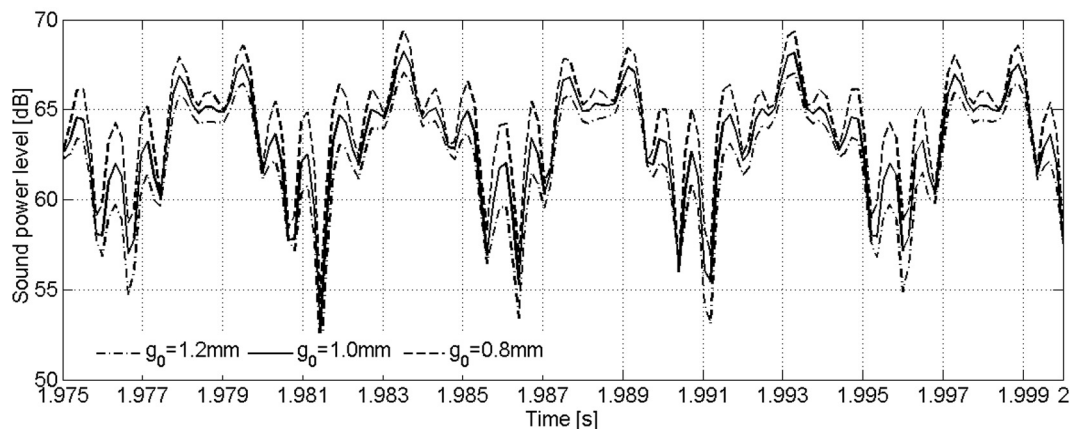


Fig. 10. Sound power level radiated by outer surface of the stator in the case of the different nominal air gap thickness

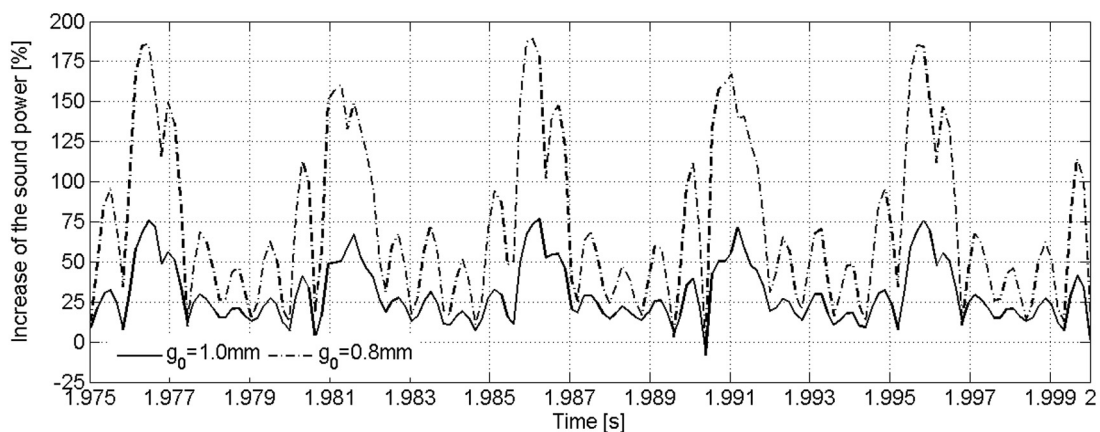


Fig. 11. Increase of the sound power radiated by outer surface of the stator due to the decrease of the nominal air gap thickness

The influence of the air gap eccentricity on the sound power of the machine was investigated as further. Obtained results are presented in Figs. 12, 13 and 14. The upper parts of these figures show the time dependences of the sound power level radiated by outer surface of the stator for different nominal air gap thicknesses and values of the parameter  $\delta = 0, 0.2$  and

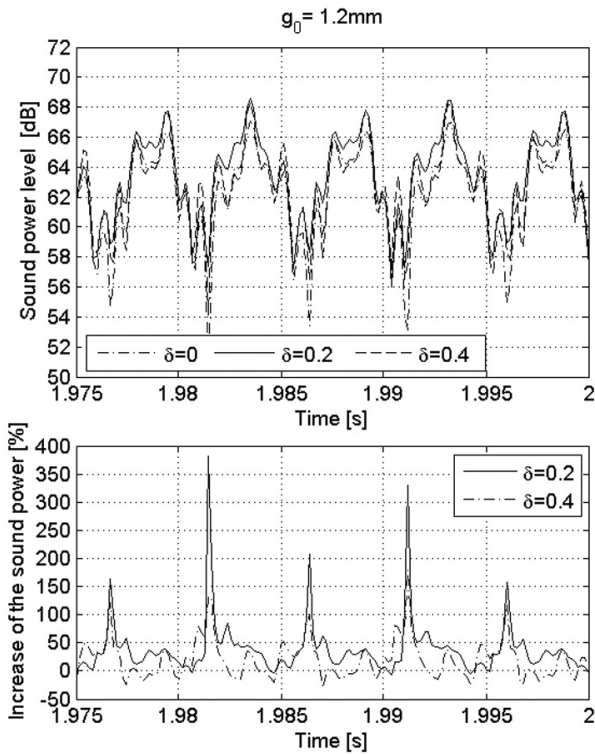


Fig. 12. Influence of the air gap eccentricity on the sound power radiated by stator, nominal air gap thickness 1.2 mm

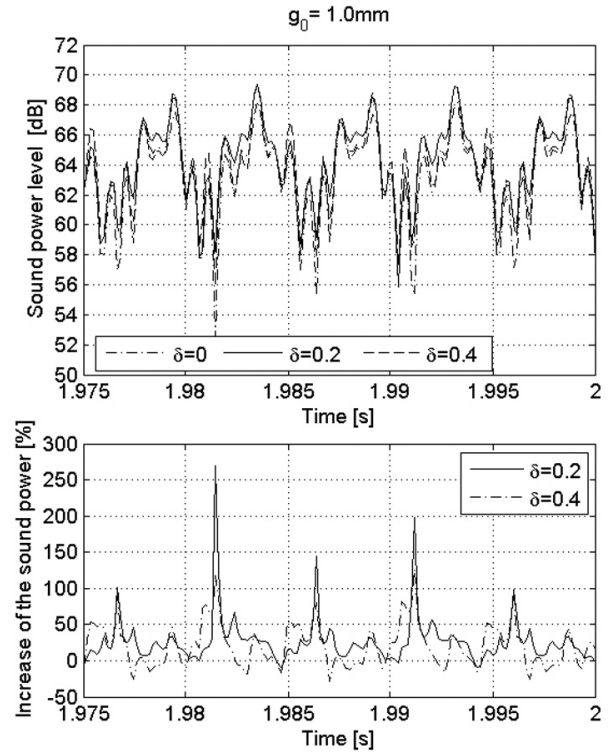


Fig. 13. Influence of the air gap eccentricity on the sound power radiated by stator, nominal air gap thickness 1.0 mm

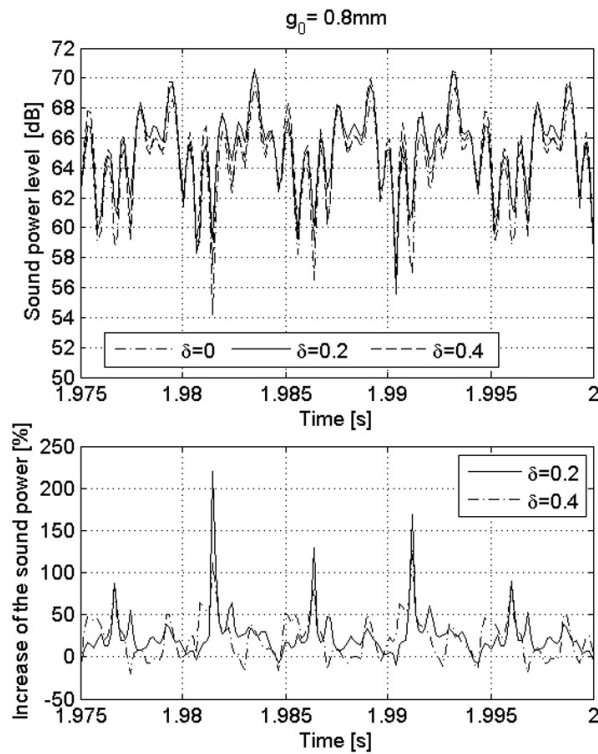


Fig. 14. Influence of the air gap eccentricity on the sound power radiated by stator, nominal air gap thickness 0.8 mm

0.4. The bottom parts of these figures compare the sound power of the machine in the case of the air gap eccentricity with the sound power of the machine in the case of the symmetric air gap. It is obvious, from these figures that the air gap eccentricity increases the sound power of the machine especially around local minimums of the time dependences of the sound power level. It is interesting that the increase of the sound power in these areas is slightly larger for  $\delta = 0.2$  than  $\delta = 0.4$ . This can be attributed to the debit of the degree of the saturation of the magnetic circuit of the machine in the vicinity of the minimal air gap thickness, which is greater in the case of  $\delta = 0.4$  than in the case  $\delta = 0.2$ . This fact confirmed by the comparison of the curves, which describe the increase of the sound power of the machine due to air gap eccentricity. The degree of saturation of the magnetic circuit of the machine is greater in the case of  $g_0 = 0.8$  mm than in the case  $g_0 = 1.0$  or  $1.2$  mm too, hence the local maximums of the curves, which describe the increase of the sound power of the machine due to the air gap eccentricity, decrease significantly less for  $\delta = 0.4$  than for  $\delta = 0.2$  with decreasing nominal air gap thickness.

In summary the nominal air gap thickness has slightly greater influence on the sound power of the machine than eccentricity of the air gap, because reduction of the nominal thickness of the machine increase magnitude of the magnetic forces along the entire circumference of the stator winding of the machine, whereas the air gap eccentricity increase the magnetic forces around minimal air gap thickness only, as Fig. 8 shows. Nevertheless the air gap eccentricity must not be neglected, because the radial components of the magnetic forces which act on the stator and the rotor winding of the machine are not cancelled out each other and the resulting magnetic force (unbalanced magnetic pull) causes additional load of the rotor of the machine.

## **5. Conclusions**

The calculation procedure of the dynamic response of the rotating electrical machine stator, which is excited by the magnetic forces, was presented. The special attention was paid to the computational model of the magnetic forces that act on the stator winding of the machine, because application of the numerical computational model of the magnetic field, based on solution of the coupled electromagnetic problem by finite element method, is not quite common yet. New approach was used also in the modelling modal properties of the stator pack.

The proposed computational model of the dynamic response of the rotating electrical machine stator excited by the magnetic forces was used to investigation of the influence of the nominal air gap thickness and the air gap eccentricity on the sound power of the machine. Obtained results show that the nominal air gap thickness has slightly greater influence on the sound power of the machine than the eccentricity of the air gap, because reduction of the nominal thickness of the machine increase magnitude of the magnetic forces along the entire circumference of the stator winding of the machine, whereas the air gap eccentricity increase the magnetic forces around the minimal air gap thickness only. The influence of the saturation effect of the stator and the rotor winding core on the sound power of the machine was demonstrated too.

The computational model of the dynamic response of the machine on the magnetic forces will be further completed by the rotor. This enhancement allows to include flexibility of the rotor and the bearing pedestals to the calculation and enables also to study the influence of the air gap eccentricity on the additional loads of the bearings of the rotor.

## **Acknowledgements**

This work was supported by grant project FSI-S-11-11/1190.

## **References**

- [1] ANSYS, Inc., Documentation for ANSYS 14.0, Canonsburk, 2011.
- [2] Arkkio, A., Analysis of induction motors based on numerical solution of the magnetic field and circuit equations, *Acta Polytechnica Scandinavia*, 1987, pp. 1–97.
- [3] Boldea, I., Nasar, S., *Induction machine hand book*, CRC Press, Boca Raton, 2001.
- [4] Burakov, A., Modelling the unbalanced magnetic pull in eccentric-rotor electrical machines with parallel windings, Helsinki University of Technology, 2007, pp. 1–70.
- [5] Carlson, R., da Silva, C. A., Sadowski, N., Lefevre, Y., Lajoie-Mazenc, M., An analysis of inter-bar Currents on a polyphase cage induction motor, *Thirty-Sixth IAS Annual Meeting 2*, 2001, pp. 721–728.
- [6] Cermer, L., Heckl, M., Peterson, B. A. T., *Structure-borne sound — Structural vibrations and sound radiation at audio frequencies*, Springer-Verlag Berlin Heidelberg, 2005.
- [7] Dušek, D., Solodyankin, K., The influence of the stiffness of the stator winding on the modal properties of the rotating electrical machines, *Elektrorevue*, Brno, 2010, pp. 1–5. (in Czech)
- [8] Faiz, J., Ebrahimi, B. M., Mixed fault diagnosis in three-phase squirrel-cage induction motor using analysis of air gap magnetic field, *Progress in Electromagnetics Research* 64 239–255.
- [9] Fengge, Z., Ningze, T., Fengxiang, W. Analysis of vibration modes for large induction motor, *Proceedings of the 8<sup>th</sup> International Conference on Electrical Machines and Systems*, 2005, pp. 64–67.
- [10] Gerlando, D. A., Foglia, G. M., Perini, R., Analytical modelling of unbalanced magnetic pull in isotropic electrical machines, *18<sup>th</sup> International Conference on Electrical Machines*, Vilamoura, Portugal, 2008, pp. 1–6.
- [11] Guo, D., Chu, F., Chen, D., The unbalanced magnetic pull and its effects on vibration in three-phase generator with eccentric rotor, *Journal of Sound and Vibration* 254 (2) (2002) 297–312.
- [12] Lundström, N. L. P., Aidanpää, J. O., Dynamic consequence of electromagnetic pull due to deviations in generator shape, *Journal of Sound and Vibration* 301 (1–2) (2007) 207–225.
- [13] Neumayer, F., Harb, W., Hauzendorfer, W., Ramsauer, F., Simulation and measurement of the vibration of hydro generator stators, *Hydrovision 2011 Conference*, Moscow, Russia, 2011, pp. 1–10.
- [14] Pennacchi, P., Computational model for calculating the dynamical behaviour of generators caused by unbalanced magnetic pull, *Journal of Sound and Vibration* 312 (1–3) (2008) 332–353.
- [15] Podzemný, Z., Creation of database of stator core stiffness of rotating electrical machines, Brno, 2013, pp. 1–85, available from: <http://www.vutbr.cz/studium/zaverecne-prace>. (in Czech)
- [16] Roivainen, J., Unit-Wave response-based modelling of the electromechanical noise and vibrations of electrical machines, Helsinki University of Technology, Helsinki, 2009, pp. 1–184.
- [17] Tenhunen, A., Finite-element calculation of unbalanced magnetic pull and circulating current between parallel windings in induction motor with non-uniform eccentric motor, *Proceedings Electric Power Applications* 150 (6) (2003) 751–756.
- [18] Yang, T., Libing, Z., Li, Langru, Parameters and performance calculation of induction motor by nonlinear circuit-coupled finite element analysis, *International Conference on Power Electronics and Driven Systems*, Taipei, 2009, pp. 979–984.
- [19] [http://www.steelnumber.com/en/stell\\_composition\\_eu.php?name\\_id=1930](http://www.steelnumber.com/en/stell_composition_eu.php?name_id=1930)